DOSIMETRIC STUDIES OF PROTON SOURCE TERMS AT PW LASER SYSTEMS

Maria-Ana POPOVICI[1], Romeo IONICA[2], Gheorghe CATA-DANIL[3]

This paper is a continuation of the preliminary dosimetric evaluation of source terms at PW laser systems [1] - the proton case. The main acceleration mechanisms and the associated characteristics of the accelerated proton beams were briefly presented. FLUKA and GEANT4 Monte Carlo transport codes were used to compute absorbed doses due to three proton beams of well defined energy and spatial distribution in a simplified geometry. "All particle" fluence maps and secondary energy spectra were used for a comparative discussion of the proton sources.

Keywords: PW lasers, radiation protection, Monte Carlo simulation, FLUKA, GEANT4, dose evaluation.

1. Introduction

Laser driven acceleration of protons and heavy ions is currently attracting high interest due to its expanding field of actual / potential medical and scientific applications: ion beam therapy, proton radiography, production of radioisotopes, fast ignition in inertial confinement fusion, etc. The new ELI-NP 2x10 PW laser facility [2] will host proton/ion acceleration experiments that are expected to bring the ultra-compact, affordable laser accelerator closer to reality. The radiological protection study at such experiments relies on the source terms, which, in this case, are not known beforehand.

This paper is a continuation of the dosimetric study we carried out for some typical electron source terms and reported in [1]. It concerns laser-accelerated proton sources over a range of laser intensities in the relativistic and ultra-relativistic regimes. The paper also contains a brief presentation of the proton acceleration mechanisms we identified in literature and the corresponding characteristics of the beams.

[1] Lecturer , Physics Dept., University POLITEHNICA of Bucharest, Romania, email: popovici@physics.pub.ro
[2] Lecturer , Physics Dept., University POLITEHNICA of Bucharest, Romania, email: r_ionica@physics.pub.ro
[3] Prof., Physics Dept., University POLITEHNICA of Bucharest, Romania, email: cata-danil@physics.pub.ro

2. Proton acceleration mechanisms

The production and acceleration of positively charged particles (protons and heavy ions) are mainly determined by the behaviour of the electron distributions produced by ultra-high intensity laser pulses incident on different types of targets. Although it is physically possible, direct acceleration requires super ultra-high laser pulse intensities ($> 5\times10^{24}$ W/cm^2), which makes this type of experiments difficult considering that the world record value of $2\cdot10^{22}$ W/cm^2 achieved with the TRIDENT laser system, at Los Alamos National Laboratory, USA, in 2008 has not been surpassed.

Protons and heavy ions result from the impurities of the target material/materials due to the contamination of the target surface with hydrocarbons and water vapors. Unless special target treatment techniques in vacuum are applied, such contamination will always exist and any laser acceleration of charged particle experiment will result in the production of energetic protons/heavy ions.

After 2000 the record proton kinetic energy of 58 MeV obtained by Snavely, a. o. [3] at Lawrence Livermore National Laboratory was not surpassed until 2011 when Gaillard a.o. [4] reported a new record of 67.5 MeV which, in its turn, was bettered in 2013, when the highest proton energy observed so far in a proton laser acceleration experiment, 160 MeV, was obtained with the TRIDENT laser system, at Los Alamos National Laboratory [5].

The main proton/heavy ion acceleration mechanisms described in literature are the following:

1. *Target Normal Sheath Acceleration* (TNSA) - the electrons of the plasma created at the incidence (hot) side of a target irradiated by an ultra high intensity laser pulse are accelerated through the target and leave the cold surface of the target. Once they are out, the electrons make up a sheath of negative charge at a small distance from the non-irradiated surface (a few microns). The large electric field due to electric charge separation acts on the atoms lying close to the cold side of the target and ionizes them. Positively charged particles (protons, heavy ions) resulted from these ionization processes are accelerated giving off broad energetic beams with large angular distribution [6].

2. *Coulombian explosion* (CE) - an ultra-high contrast laser pulse (to prevent ionization of the target before the laser peak) is incident on a very thin, submicronic target, transparent to the laser pulse, and it accelerates most of the electrons out of the target. The positively charged protons and heavy ions are consequently accelerated in the high intensity coulombian rejection force fields [7].

3. *Radiation pressure acceleration* RPA occurs when an ultra-high intensity and contrast laser pulse is incident on an ultrathin foil (typically of nanometer order magnitude). The radiation pressure (I / c) accelerates the target as a whole (light-sailing regime) or, if the target is "thicker" (i.e. it is larger than the the laser penetration depth), it produces the deformation of plasma, which acts as an ultradense plasma with a concave separation surface (hole boring regime). In both cases the proton/ion accelaration is aided by the lack of background plasma screening [8].

4. *Magnetic vortex acceleration* (MVA) - the laser pulse creates a channel inside the target in which large electric and magnetic fields are acting thus generating a complex energetic distribution of accelerated protons with a low divergence cuasimonochromatic longitudinal component and a broad transverse component [9].

The development of these mechanisms resulted in new acceleration mechanisms which were theoretically predicted or resulted from particle-in-cell code simulations.

Enhanced TNSA is obtained when the ultra-high contrast ($< 10^{-11}$) laser pulse interacts with hundreds of nanometers thick solid targets and it can be described in terms of adiabatic expansion of the neutral plasma. Ion acceleration will continue after the end of the laser pulse, cuasi-symmetrically from both the hot and cold side of the target, until the adiabatic cooling of the electrons occurs [10].

Breakout Afterburner Acceleration (BOA) is achieved when the ultradense target plasma becomes transparent to the laser pulse (the relativistic transparency regime). In BOA the laser pulse brings the whole electron population to relativistic energies, thus lowering the plasma frequency. The overall effect is an increase of the laser energy coupling to the particles in the interaction volume which results in a larger number of accelerated particles to higher kinetic energy. This is the mechanism which was used to obtain the record value of around 160 MeV protons at Los Alamos National Laboratory with the Trident laser [5].

The *enhanced Coulombian explosion* is a PIC predicted acceleration mechanism which could lead to monoenergetic, one directional proton beams of GeV energies. It consists in the well confined acceleration of protons externally injected in the wakefield of a Laguerre - Gaussian laser pulse. The directed Coulombian explosion is achieved by using a double layer microtarget. The Coulombian explosion of the first layer (high Z material) results in a moving electrostatic potential in which the protons of the second layer (hydrogen or hydogen compound) are accelerated [11].

3. General characteristics of the proton beams obtained by laser acceleration

TNSA is the most thorougly investigated acceleration mechanism both teoretically and experimentally. The protons/ions obtained by this type of acceleration generally have a broad spectral energy distribution with values up to tens of MeV. The protons/ions lying close to the cold side of the target are subject to higher field gradients and they are accelerated preferentially, thus screening the inner protons. This differentiated acceleration causes the broad distribution of the accelerated particles. The same effect may be due to inhomogeneous charge distribution in the electronic sheath which creates inhomogeneous accelerating fields.

Theoretical expressions of the proton energy distribution function and of the proton maximum energy in TNSA were obtained within the isothermal plasma dilation model [12, 13]:

$$\frac{\mathrm{d}N_\mathrm{p}}{\mathrm{d}E} = \frac{n_{\mathrm{p},0} c_\mathrm{s} t_\mathrm{acc}}{\sqrt{2 k_\mathrm{B} T_\mathrm{e} E}} \exp\left(-\sqrt{\frac{2E}{k_\mathrm{B} T_\mathrm{e}}}\right), \tag{1}$$

where the hypothesis of equilibrium plasma quasi-neutrality is used: $n_{\mathrm{e},0} = n_{\mathrm{p},0}$, the ion speed of sound is $c_\mathrm{s} = \sqrt{k_\mathrm{B} T_\mathrm{e} / m_\mathrm{p}}$, T_e - the temperature of the hot electrons, t_acc - the proton acceleration time. The maximum proton energy is given by the equation:

$$E_\mathrm{max} \approx 2 k_\mathrm{B} T_e \ln\left(\tau + \sqrt{\tau^2 + 1}\right), \tag{2}$$

where $\tau = \omega t \Big/ \sqrt{2\exp(1)}$ is a nondimensional time variable and $\omega_\mathrm{p} = \sqrt{n_{\mathrm{e},0} e^2 \big/ \varepsilon_0 m_\mathrm{p}}$ is the proton plasma frequency.

Equations (1) and (2) actually describe the scaling proposed by Fuchs et al. [13] who replaced the time (which in the original theory appeared as a continuous infinite variable) by a finite acceleration time. This is equivalent to introducing a phenomenological cutoff. t_acc is determined by the laser pulse duration, τ_L, and it was demonstrated that an equation which fits the experimental data correctly is $t_\mathrm{acc} \approx 1.3\tau_\mathrm{L}$.

A scaling law of the maximum proton energy was derived from the experimental data: $E_\mathrm{max} \propto \sqrt{I}$ [13], where I is the laser intensity. The TNSA protons are characterized by relatively large angular distributions, the divergence half angle can be up to 30° [14]. They are obtained as bunches with an ultra short duration: picosecond bunches result in a typical TNSA experiment (as compared

to nanosecond bunches obtained with conventional proton accelerators). Other favourable characteristics are: *high brilliance*: up to $10^{10} - 10^{13}$ protons/pulse can be scored [3], [15], *high currents* (order kA), *low emittance* [16] - the average measured value is 0.01π mm-mrad, two orders magnitude less than in conventional accelerators, *small size*: the initial dimension of the proton source can be estimated the equation $r_p = r_0 + d\,\mathrm{tg}(\theta_e/2)$, where r is the radius of the laser focal spot, d is the thickness of the spot, θ_e is the divergence of the electron beam in the target (the electrons are those which make up the sheath and accelerate the protons).

In the CE regime, PIC simulations predict broad energetic spectra of the exponential type. By replacing the target with a double layer target, in the directed Coulombian explosion regime, proton beams with at least one monochromatic, one-directional component whose maximum energy exceeds 100 MeV can be obtained [17, 18].

PIC code simulation results show that RPA is a very efficient mechanism which can lead to monoenergetic proton beams of hundreds of MeV (up to GeV) energy, with very low divergence, just as in the conventional accelerators. In this regime, the maximum proton energy scales with the laser pulse energy, as Esirkepov et al. showed by aplying multi-parametric PIC simulations [19]. However the setup of such an experiment can be quite restrictive: high intensity of the laser pulse ($> 10^{22}$ W/cm^2), ultra-high contrast (10^{-12} or less), circular polarization for increased efficiency, ultra-thin targets (order nanometers) [8, 19, 20].

3. Proton source terms

We implemented a set of three source terms of protons (SP1 - SP3) in FLUKA [21, 26] and GEANT4 [22].

SP1 is a uniform energetic distribution in which the proton energy values lie in the 0 – 100 MeV interval, with the same probability. This is an estimate which points to an upper limit of the experimental results achieved in the first decade of the 21-st century in laser proton acceleration by TNSA. [23] The spatial distribution we considered is broad, within a cone whose opening angle is 40°, as suggested by the experimental results and the PIC simulations [14].

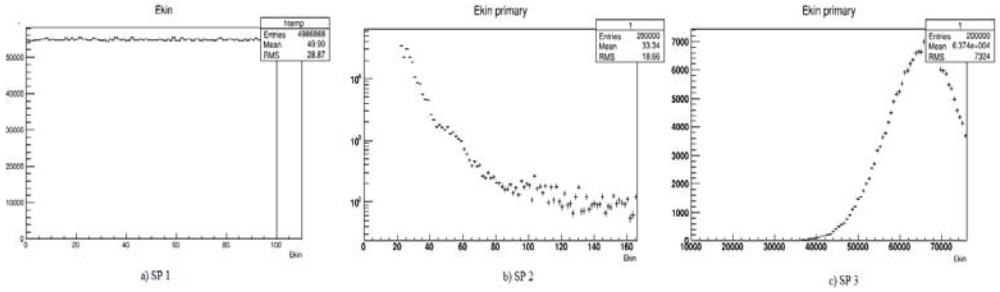

Fig. 1. Proton source terms generated by the GPS module of GEANT4

SP2 describes the record experimental results for proton acceleration achieved at Los Alamos National Laboratories. The laser pulse was focused on a plastic CH_2 solid target, 400 nm thick to produce a peak intensity of $1.6\times10^{21}\ \mathrm{W/cm^2}$ (BOA regime). The energetic spectral data were obtained by digitizing the published spectra. The simulated beam has a broad spatial distribution in a cone with total opening angle of 40° [5].

SP3 was defined according to the PIC simulation results [24] which show that a peak intensity of $2.14\times10^{23}\ \mathrm{W/cm^2}$ in the focal spot can generate in a microtarget embedded in subdense plasma a proton beam with a maximum energy of 76 GeV, in a secvential mechanism of acceleration by radiation pressure and bubble regime. We fit published data to a Gaussian energetic distribution with an average value of 66 GeV, FWHM of 9 GeV and a cutoff energy at 76 GeV. The beam divergence was 3°.

4. Results

The current dosimetric simulation study was conducted in the same simplified geometry described in [1]. Fluka physics settings (default, thresholds, low energy neutron and ion transport) were similar for beam particles lying in similar energy ranges. The radiation terms described above were implemented in three FLUKA SOURCE subroutines: pro-100MeV.f, exper-histo.f and gauss-cutoff.f. Their outputs were crosschecked with the energy distributions given by the General Particle Source (GPS) module which was activated in the DOSE program written in GEANT4. The dose was accumulated directly from energy deposition at each step in the selected volume. The energy distributions of the source terms are presented in Figure 1, as output of GPS. In GEANT4 the physics of the interaction processes is according to the QBBC dedicated physics list. The hadronic processes of the protons and neutrons are modelled by hElasticCHIPS

(elastic) and Binary Cascade (0-1.5GeV), Bertini Cascade (1-12GeV) and FTFP (3GeV-100TeV) [25].

Table 1 contains the results of our parallel FLUKA/GEANT4 dose calculations for the main components of the simulation setup: detector, interaction chamber and its window. They are in good general agreement with each other. It can be seen that SP1 (the estimated energy distribution function [23]) gave similar results with SP2 (the experimental one, corresponding to the highest maximum energy) which suggests that it is safe to use it when performing radioprotection calculations at laser driven proton acceleration experiments when the maximum proton energy does not surpass 200 MeV. SP3 is a collimated beam of relatively small angular width, which explains the lowest energy deposited in the interaction chamber with which it does not interact directly.

Tabel 1

Dose (pGy/ primary proton) due to all particles generated by the implemented proton source terms and associated relative errors (%)

		SP1 - Dose (pGy/proton)	**SP2 - Dose (pGy/proton)**	**SP3 - Dose (pGy/proton)**
Detector	FLUKA	**3.709E-03 0.47%**	**2.797E-03 0.18%**	**4.056E+01 0.14%**
	GEANT4	**3.752E-03 0.02%**	**3.835 E-03 1.7%**	**4.003E+01 0.3**
Interaction chamber	FLUKA	**2.323E-03 0.03%**	**1.819E-03 0.008%**	**7.375E-04 0.26%**
	GEANT4	**2.322E-03 0.02%**	**2.317E-03 0.07%**	**8.713E-04 0.9%**
Window	FLUKA	**2.827E-01 0.09**	**3.031E-01 0.02%**	**2.445E-01 0.7%**
	GEANT4	**2.811E-03 0.09%**	**2.829E-01 0.3%**	**2.851E-01 0.2%**

Also, the deposited dose in the "detector" region is highest, since most of the energetic protons pass through the thin window with unaltered energy and interact directly with the "detector" region. That itself is not too large (10cm linear dimension), and thus FLUKA reports a 93% of the primary energy leaving the sistem.

In FLUKA, we scored the fluence due to all particles in a Cartesian mesh spanning all the geometry. The 2D map representations of the results for SP1 and

SP2 are given in Figure 2, in a horizontal plane, slicing the geometry at the laser beamline height. They were obtained by FLAIR, the graphical advanced interface of FLUKA [27]. Notice that the ranges covered by the "all particle" fluence values are similar. Along with the absorbed dose results found in Table 1, the fluence maps similarity supports the idea that SP1 is a good estimate of a broad energy distribution proton source term to be used for dose calculations when the proton energies are less than 200 MeV (a range which is also important for medical applications).

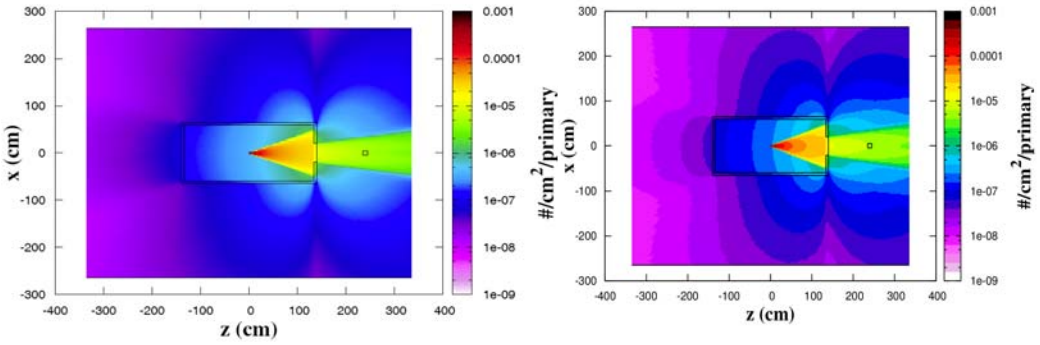

Fig. 2. All particle fluence (particles/cm^2/primary proton) in the Oxz plane at y = 0: a) generated by SP1; b) generated by SP2. The source is placed at the center of the interaction chamber.

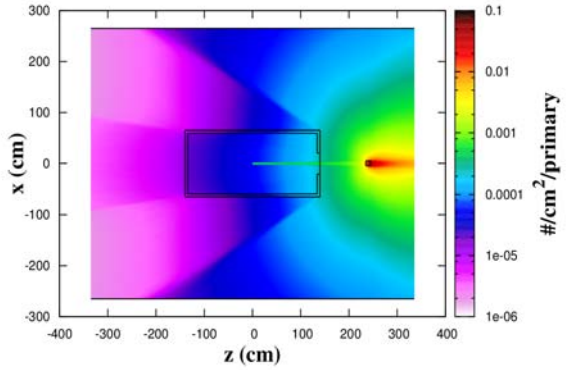

Fig. 3. All particle fluence (particles/cm^2/primary proton) generated by SP3 in the Oxz plane at y = 0. The source is placed at the center of the interaction chamber

For both SP1 and SP2 terms, the loss of primary proton energy is mainly due to the stopping power of the materials with which they interact (aluminum, copper), around 83%. SP2 also has a very small component of electromagnetic shower, around 1%. The energetic protons escape the system (our simplified simulation setup does not include walls). Only 15% (aproximately) of the beam energy is escaping the system for SP1 and SP2, as compared to 93%, for SP3, which is a collimated distribution of highly energetic protons. This can be seen in Fig. 3, which gives the map of "all particles" fluence distribution throughout the geometry. The loss of energy due to stopping power for SP3 is small, around 1.5%.

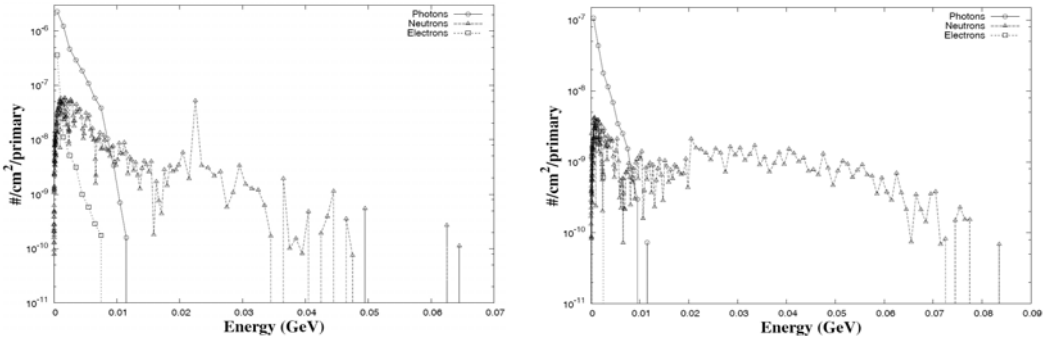

a) b)

Fig. 4. Energy spectra of secondaries produced by SP1, scored through the detector -air interface: a) at the front (hot) face of the detector, in the backward direction with respect to the incidence of the beam protons; b) at the back (cold) face of the detector, in the forward direction.

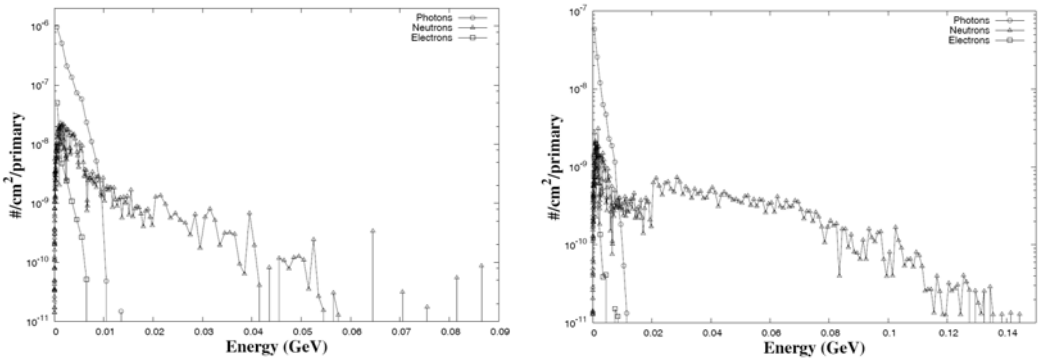

a) b)

Fig. 5. Energy spectra of secondaries produced by SP2, scored through the detector -air interface: a) at the front (hot) face of the detector, in the backward direction with respect to the incidence of the beam protons; b) at the back (cold) face of the detector, in the forward direction.

To describe the secondary radiation field, we scored the energy spectra at the front (hot) detector -air interface and at the back (cold) one. The results are presented in Figures 4 - 6, for SP1 - SP3. As expected, in the intermediate energy interaction regime (SP1 and SP2), the dominant secondaries are the neutrons. Evaporation neutrons produced at smaller energies have an isotropic distribution and this explains why there is a quantitatively important neutron component both in the backward and forward direction with respect to the proton incidence. The reason why SP2 produces less such neutrons is that the experimental energy distribution which we sampled misses protons with energy less than 20 MeV (see Figure 1b). Figures 4 and 5 also reveal a forward peaked neutron yield, due to higher energy nuclear reactions. Figure 6a shows a small production of low energy neutrons in the volume of the detector region, which leave it in the backward direction. The high energy interactions of protons produce significant amounts of neutrons, photons, electrons, and muons in the forward direction, as one can see in Figure 6b.

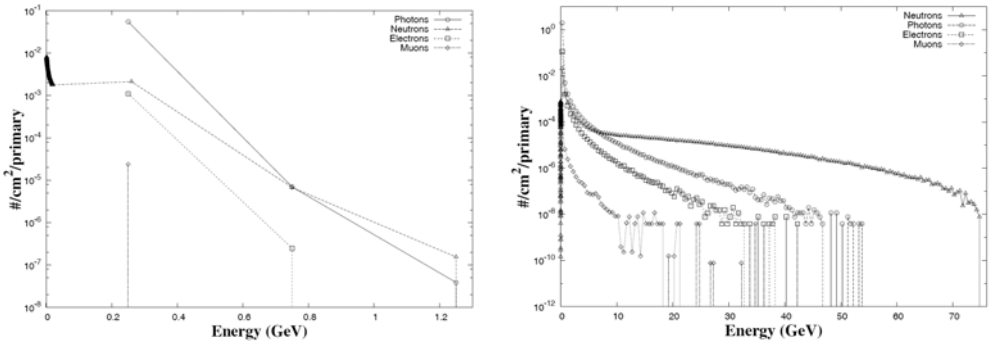

a) b)

Fig. 6. Energy spectra of secondaries produced by SP3, scored through the detector -air interface: a) at the front (hot) face of the detector, in the backward direction with respect to the incidence of the beam protons; b) at the back (cold) face of the detector, in the forward direction.

FLUKA statistics show that in the entire simulation setup the most important secondaries generated in inelastic interactions per beam proton of SP1 or SP2 are photons ($\approx$ 40%), protons ($\approx$ 33%) and neutrons ($\approx$ 15%). The statistics for SP3 reveals neutrons ($\approx$ 34%), photons ($\approx$ 21%), protons ($\approx$ 17%) and other secondaries like pions (positive, negative and neutral, an overall percentage of $\approx$ 17%), which are not present at low energies.

5. Conclusions

In the current Monte Carlo simulation study of proton sources at PW laser acceleration experiments, three energy distributions were sampled: an estimated uniform one, which covers existing and expected TNSA experimental results, a

BOA experimental result (which set a record in proton acceleration) and finally, a PIC simulation derived energy distribution. Together, they span a wide range of proton energy values, from zero to tens of GeV. Parallel FLUKA and GEANT4 calculations showed that the results were in general good agreement over that range.

Similarly to the electron case, "all particle" fluence maps generated by proton beams reveal that the energy and spatial distributions *combined* determine the secondary radiation fields at the experimental site. PIC simulations predict that high energy distributions of protons are usually collimated, and the radioprotection issues are similar to those at the conventional accelerators. According to our calculations, smaller energy distributions, with a broad spatial extension can pose more problems. This is explained by the large number of secondaries with a broad (sometimes isotropic) distribution generated by the interactions of the primary protons (also broadly distributed) in the thick walls of the interaction chamber.

The secondary energy spectra reported here concern only those particles which are produced inside the "detector" volume and leave it in the backward and forward direction. SP1 and SP2 produce a comparable amount of secondaries in both directions. The most energetic ones are neutrons. For SP3, secondary neutrons are forwardly peaked and cover the whole range of the primary spectrum, thus requiring special measures for radioprotection. In future we will use these proton source terms for a radiological characterization of a real laser accelerator experimental facility.

Acknowledgement

This work was supported by a grant in the programme: CAPACITIES/RO-CERN, project type: ELI-NP, E/04 HHGDE, project number 04/27.06.2014.

R E F E R E N C E S

[1]. *M. A. Popovici, R. Ionica, Gh. Cata - Danil*, Preliminary dosimetric evaluation of electron source terms at PW laser systems, U.P.B. Sci.Bull. A, **vol. 1**, no.1, 2015, pp 249-263

[2]. *N. V. Zamfir,* Nuclear Physics with 10PW laser beams at Extreme Light Infrastructure – Nuclear Physics (ELI–NP), Eur. Phys. J. Special Topics, vol 223, 2014, pp. 1221-1227

[3]. *R. A. Snavely, M. H. Key, S. P. Hatchett, T. E. Cowan, M. Roth, T. W. Phillips, M. A. Stoyer, E. A. Henry, T. C. Sangster, M. S. Singh, S. C.Wilks, A. MacKinnon, A. Offenberger, D. M. Pennington, K. Yasuike, A.B. Langdon, B. F. Lasinski, J. Johnson, M. D. Perry, E. M. Campbell*, Intense high energy proton beams from petawatt – laser irradiation of solids, Phys. Rev. Lett., **vol. 85**, 2945, 2000

[4]. S. A. *Gaillard; T. Kluge,K. A. Flippo, M. Bussmann, B. Gall, T. Lockard, M. Geissel, D. T. Offermann; M. Schollmeier, Y. Sentoku, T. E. Cowan,* Increased laser-accelerated proton energies via direct laser-light-pressure acceleration of electrons in microcone targets, Physics of Plasmas, **vol. 18**, no. 5: 056710, 2011

[5]. *B. M. Hegelich, D. Jung, B. J. Albright, M. Cheung, B. Dromey, D. C. Gautier, C. Hamilton, S.Letzring, R. Munchhausen, S. Palaniyappan, R. Shah, H.-C. Wu, L. Yin1, J. C. Fernández*, 160 MeV laser accelerated protons from CH2 nanotargets for proton cancer therapy, arXiv: 1310. 8650 v1 [physics.plasm-ph], 2013

[6] *S. C. Wilks, A. B. Langdon, T. E. Cowan, M. Roth, M. Singh, S. Hatchett, M. H. Key, D. Pennington, A. MacKinnon, R. A. Snavely*, Energetic proton generation in ultraintense laser-solid interactions, Phys. Plasmas, **vol. 8**, 2001, pp 542–549

[7] *S. S. Bulanov, A. Brantov, V. Yu. Bychenkov, V. Chvykov, G. Kalinchenko, T. Matsuoka, P Rousseau, V. Yanovsky, D. W. Litzenberg, K. Krushelnick, A. Maksimchuk*, Accelerating monoenergetic protons from ultrathin foils by flat-top laser pulses in the directed-Coulomb-explosion regime, Phys. Rev. E, 78, 2008, 026412

[8] *T. Esirkepov, M. Borghesi, S. V. Bulanov, G. Mourou, T. Tajima*, Highly efficient relativistic ion generation in the laser-piston regime, Phys. Rev. Lett, **92**, 175003, 2004.

[9] *S. S. Bulanov, V. Yu, Bychenkov, V. Chvykov, G. Kalinchenko, D. W. Litzenberg, T. Matsuoka, G. R. Thomas, L. Willingale, V. Yanovsky, K. Krushelnick, A. Maksimchuk*, Generation of GeV protons from 1 PW laser interaction with near critical density targets, Phys. Plasmas, **17**, 043105, 2010

[10] *A. A. Andreev, S. Steinke, T. Sokollik, M. Schnurer, S. Ter Avetsiyan, K. Y.Platonov, and P. V. Nickles*, Optimal ion acceleration from ultrathin foils irradiated by a proled laser pulse of relativistic intensity, Physics of Plasmas, **16**, 013103, 2009.

[11] *X. Zhang, B. Shen, L. Zhang, J. Xu, X. Wang, W. Wang, L. Yi, Y. Shi*, Proton Acceleration in Underdense Plasma by UltraintenseLaguerre-Gaussian Laser Pulse, arXiv:1407.6467v1, [physics.plasm-ph], 2014

[12] *P. Mora*, Plasma expansion into a vacuum, Phys. Rev. Lett., **90**, 185002, 2003.

[13] *J. Fuchs, P. Antici, E. d'Humières, E. Lefebvre, M. Borghesi, E. Brambrink, C. A. Cecchetti, M. Kaluza, V. Malka, M. Manclossi, S. Meyroneinc, P. Mora, J. Schreiber, T. Toncian, H. Pépin, P. Audebert*, Laser-driven proton scaling laws and new paths towards energy increase, Nat. Phys., **2**, 48, 2006.

[14] *F. Nürnberg, M. Schollmeier, E. Brambrink, A. Blaževic, D. C. Carroll, K. Flippo, D. C. Gautier, M. Geißel, K. Harres, B. M. Hegelich, , O. Lundh, K. Markey, P. McKenna, D. Neely, J. Schreiber,M. Roth*, Radiochromic film imaging spectroscopy of laser accelerated proton beams, Rev. Sci. Instrum., **80**, 033301, 2009

[15] *S. P. Hatchett, C. G. Brown, T. E. Cowan, E. A. Henry, J. S. Johnson, M. H. Key, J. A. Koch, B. Langdon, B. F. Lasinski, R. W. Lee, A. J. Mackinnon, D. M. Pennington, M. D. Perry, T. W. Phillips, M. Roth, T. C. Sangster, M. S. Singh, R. A. Snavely, M. A. Stoyer, S. C. Wilks, K. Yasuike*, Electron, photon, and ion beams from the relativistic interaction of petawatt laser pulses with solid targets, Phys. Plasmas, 7, 2076, 2000

[16] *T. E. Cowan, J. Fuchs, H. Ruhl, A. Kemp, P. Audebert, M. Roth, R. Stephens, I. Barton, A. Blaževic, E. Brambrink, J. Cobble, J. Fernández, J.-C. Gauthier, M. Geißel, M. Hegelich, J. Kaae, S. Karsch, G. P. Le Sage, S. Letzring, M. Manclossi, S. Meyroneinc, A. Newkirk, H. Pépin, N. Renard-LeGalloudec*, Ultralow Emittance, Multi-MeV Proton Beams from a Laser Virtual-Cathode Plasma Accelerator. Phys. Rev. Lett., **92**, 204801, 2004

[17] *H. Schwoerer, S. Pfotenhauer, O. Jäckel, K.-U, Amthor, B. Liesfeld, W. Ziegler, R. Sauerbrey, K. W. D. Ledingham, T. Esirkepov*, Laser-plasma acceleration of quasi-monoenergetic protons from microstructured targets, Nature, 439, 445, 2006

[18] *B. M. Hegelich, B. J. Albright, J. Cobble, K. Flippo, S. Letzring, M. Paffett, H. Ruhl, J. Schreiber, R. K. Schulze, J. C. Fernández*, Laser acceleration of quasi-monoenergetic MeV ion beams, Nature, 439, 441, 2006.

[19] *T.Esirkepov, M. Yamagiwa, T. Tajima T*, Laser Ion-Acceleration Scaling Laws Seen in Multiparametric Particle-in-Cell Simulations, Phys. Rev. Lett. vol. 96, 2006, pp. 105001

[20] *Klimo, J. Psikal, J. Limpouch, and V. T. Tikhonchuk*, Monoenergetic ion beams from ultrathin foils irradiated by ultrahigh-contrast circularly polarized laser pulses. Phys. Rev. ST Accel. Beams, 11, 031301, 2008.

[21] *A. Ferrari, P.R. Sala, A. Fasso`, J. Ranft,* FLUKA: a multi-particle transport code" CERN-2005-10, 2005, INFN/TC_05/11, SLAC-R-773

[22] *S. Agostinelli, J. Allison, K. Amako, J. Apostolakis, H. Arauho, et al*. (GEANT4 Collaboration) Geant4: a simulation toolkit. Nucl. Instr. Methods, A506, 2003, pp. 250-303; Web site: http://geant4.cern.ch

[23]. ELI - Extreme Light Infrastructure WHITEBOOK, Science and Technology with Ultra-Intense Lasers, Editors G.A. Mourou, G. Korn, W. Sandner, J.L. Collier Editors, at THOSS Media GmbH, (2011), http://www.eli-beams.eu/wp-content/uploads/2011/08/ELI-Book_neues_Logo-edited-web.pdf

[24] *Xi. Zhang, B. Shen, L. Ji, F. Wang, M. Wen, W. Wang , J. Xu , Yahong Yu*, Ultrahigh energy proton generation in sequential radiation pressure and bubble regime, Phys. Plasmas, 17 (12), 123102, 2010

[25] Physics Reference Manual, http://geant4.cern.ch/support/userdocuments.shtml

[26] *T.T. Böhlen, F. Cerutti, M.P.W. Chin, A. Fassò, A. Ferrari, P.G. Ortega, A. Mairani, P.R. Sala, G. Smirnov, V. Vlachoudis,* The FLUKA Code: Developments and Challenges for High Energy and Medical Applications, Nuclear Data Sheets vol. 120, 2014, pp. 211-214

[27] *V.Vlachoudis* "FLAIR: A Powerful But User Friendly Graphical Interface For FLUKA" Proc. Int. Conf. on Mathematics, Computational Methods & Reactor Physics (M&C 2009), Saratoga Springs, New York, 2009